CI&CEQ
Chemical Industry & Chemical Engineering Quarterly

Available on line at
Association of the Chemical Engineers of Serbia AChE
www.ache.org.rs/CICEQ

Chem. Ind. Chem. Eng. Q. 27 (1) 69–78 (2021) CI&CEQ

RURU FU[1]
ZHUANGZHANG HE[1]
SHIKAI QIN[1]
QINGZE JIAO[1,2]
CAIHONG FENG[1]
HANSHENG LI[1]
YUN ZHAO[1]

[1]School of Chemistry and Chemical Engineering, Beijing Institute of Technology, Beijing, PR China
[2]School of Materials and Environment, Beijing Institute of Technology, Zhuhai, Guangdong, PR China

SCIENTIFIC PAPER

UDC 66.092-097.3:678.065:628

LIGHT OLEFIN PRODUCTION USING THE MIXTURE OF HZSM-5/MCM-41 AND γ-Al_2O_3 AS CATALYSTS FOR CATALYTIC PYROLYSIS OF WASTE TIRES

Article Highlights

- The mixtures of γ-Al_2O_3 and HZSM-5/MCM-41 were used as catalysts
- The mixed catalysts have micro-, meso- and macropores
- The catalysts were used to catalyze the pyrolysis of waste tires
- The selectivity to light olefins was enhanced by the introduction of γ-Al_2O_3

Abstract

In this paper, micro-mesoporous HZSM-5/MCM-41 zeolites were prepared by a two-step hydrothermal method using commercial HZSM-5 with two different silica/alumina ratios (38 and 50) as starting materials. The structures, morphologies and acidity of as-prepared zeolites were analyzed using XRD, FT-IR, SEM, N_2-adsorption/desorption and NH_3-TPD. The HZSM-5/MCM-41 zeolites combined the acidity of microporous HZSM-5 with the pore advantages of mesoporous MCM-41. Mesopores and microspores of 3.34 and 0.95 nm in diameter were found to be present in HZSM-5/MCM-41 zeolites. When they were used to catalyze the pyrolysis of waste tires, the selectivity of light olefins for HZSM-5/MCM-41 prepared using HZSM-5 with the silica/alumina ratio of 50 as starting materials was 21.42%, higher than 18.43% of HZSM-5/MCM-41 synthesized using HZSM-5 with the silica/alumina ratio of 38. In order to further overcome the pore size constraints and mass transfer limitations of HZSM-5/MCM-41 zeolites for catalyzing pyrolysis of waste tires, macroporous γ-Al_2O_3 were mixed with HZSM-5/MCM-41 and used as catalysts. The selectivity to light olefins for the mixture of γ-Al_2O_3 and HZSM-5/MCM-41 prepared using HZSM-5 with the silica/alumina ratio of 50 as starting materials was 33.65%, which was obviously enhanced by the introduction of γ-Al_2O_3.

Keywords: catalytic pyrolysis, HZSM-5, light olefins, MCM-41, waste tires, γ-Al_2O_3.

Light olefins (C_2-C_4 olefins) are important basic chemical materials for producing polyolefins, which are widely applied in various fields. In recent years, the demand for light olefins has been rising and the contradiction between supply and demand will also become increasingly prominent [1]. At present, the source of light olefins is mainly petroleum as well as coal. The gradual depletion of oil and coal reserves has aroused people's interest in finding alternative sources of energy. At the same time, the number of waste tires is growing more and more with the rapid development of the automotive industry. It is very important to effectively recycle and reuse the waste tires [2]. In addition to fuel oil and aromatic compounds, light olefins can also be obtained by catalytic cracking of waste tires. In other words, waste tires could be a potential resource for the production of light olefins. However, most researchers have focused on obtaining oils rather than valuable light olefins by waste tire pyrolysis due to the low selectivity and yields of olefins [3-5]. Therefore, it is a key factor to find an effective catalyst for pyrolysis of waste tires

Correspondence: Y. Zhao, Shengtailou 330, School of Chemistry and Chemical Engineering, Beijing Institute of Technology, Liangxiang, Fangshan District, Beijing 102488, P. R. China.
E-mail: zhaoyun@bit.edu.cn
Paper received: 2 March, 2020
Paper revised: 5 July, 2020
Paper accepted: 14 July, 2020

https://doi.org/10.2298/CICEQ200302025F

to produce light olefins with high selectivity and yields [6-8].

Zeolites are the most commonly used catalysts for cracking waste tires. Salmasi *et al.* [9] studied the effect of HZSM-5 zeolites on the pyrolysis of polybutadiene rubber, and the yield of olefins was about 16.8%. Shen *et al.* [10,11] used USY and ZSM-5 catalysts for catalytic pyrolysis of waste tires, respectively. The concentrations of straight chain and cyclic olefins obtained by USY were 3.49 and 0.76%, lower than 5.80 and 21.46% of HZSM-5 in the light fractions. Some zeolites such as standard ZSM-5, nanocrystalline n-ZSM-5 and beta zeolites were proved to increase the selectivity towards monocyclic aromatics including toluene (up to 19.82%), *m*/*p*-xylene (up to 16.91%) and benzene (up to 10.28%) [12].

Commercial HZSM-5 molecular sieves and other microporous zeolites have relatively low olefin selectivity and relatively high aromatic selectivity due to the following reasons. Firsty, long and narrow micropores are not suitable for the diffusion of light olefins, as obtained light olefins continue to react to produce aromatics or even carbon deposits [13,14]. Secondly, the local acid density is so high that the resulting light olefins continue to react at strong acid sites to produce aromatics or even carbon deposits [15,16].

In order to overcome the pore size constraint of microporous zeolites, mesoporous zeolites and hierarchical zeolites with micro- and mesopores are used to catalyze the pyrolysis of waste tires.

Anh *et al.* [1,17] studied the effect of Ru/MCM--41 and Ru/MCM-48 composite catalysts on tire pyrolysis. The yield of light olefins of non-catalyst, Ru/ /MCM-41 and Ru/MCM-48 catalysts were approximately 2.5, 4.6 and 7.6%, respectively. The light olefins obtained using Ru/MCM-41 and Ru/MCM-48 were 2 and 4 times as much as non-catalyst-obtained. Additionally, the mesoporous MCM-48 gave higher selectivity of propylene than ethylene.

Witsarut *et al.* [18] studied the effect of HY/ /MCM-41 core-shell composites on waste tire pyrolysis. The HY/MCM-41 composite contains micro- and mesopores. The yields of olefins of non-catalyst, HY, MCM-41 and the HY/MCM-41 core-shell composite were 9.0, 8.1, 10.0 and 12.0%, respectively. Compared to microporous HY and mesoporous MCM-41, the HY/MCM-41 composite with both micro- and mesopores showed an increased yield of olefins. HZSM-5/MCM-41 is the most common kind of hierarchical zeolites with micro- and mesopores. Although few investigations of HZSM-5/MCM-41 have been reported for catalyzing waste tire pyrolysis, they are used as catalysts for pyrolysis of other materials. Zhao *et al.* [19] used hierarchical HZSM-5/MCM-41 for catalytic pyrolysis of rice husk. The relative abundance of olefins for HZSM-5/MCM-41 was 14.5%, higher than 10.1% of HZSM-5. Sang *et al.* [20] prepared HZSM-5/MCM-41 composite molecular sieves for catalytic cracking of *n*-decane, and the maximum selectivity of light olefins was about 21%.

Herein, hierarchical HZSM-5/MCM-41 catalysts with micro- and mesopores were synthesized by a two-step hydrothermal method using a commercial HZSM-5 zeolite as a starting material and CTAB as a template. Considering some characteristics of macroporous γ-Al_2O_3, such as large specific surface area, larger pore diameter (pore size distribution of 5-70 nm), and a certain amount of acid sites, γ-Al_2O_3 were added into HZSM-5/MCM-41 to obtain the mixed catalysts with micro-, meso- and macropores to catalyze the pyrolysis of waste tires. The effects of catalyst composition on the selectivity of light olefins for the catalytic pyrolysis of waste rubber tires were investigated.

EXPERIMENTAL

Materials

HZSM-5 zeolites (SiO_2/Al_2O_3 ratios of 38 and 50) were obtained from Nankai University Catalyst Plant. Cetyltrimethylammonium bromide (CTAB), hydrochloric acid (HCl, 2 M in water) and quartz sand (10-20 mesh and 100-200 mesh) were purchased from Sinopharm Chemical Reagent Co., Ltd. Sodium hydroxide (NaOH), ammonia chloride (NH_4Cl) and potassium bromide (KBr) were obtained from Shanghai McLean Biochemical Technology Co., Ltd. γ-Al_2O_3 was obtained from Tianjin Kevin Technology Co. Ltd. The waste rubber tires used in the experiment are black solid powders obtained by pulverizing the waste rubber tires of automobiles after removing the fiber and the iron wire.

Preparation of HZSM-5/MCM-41

A certain amount of commercial HZSM-5 zeolites (SiO_2/Al_2O_3 ratios of 38 and 50, respectively) was added into a 1.5 M NaOH solution and treated at 40 °C for 1 h. The quantitative CTAB templates (the mole ratio of SiO_2/CTAB is 4.16) were dissolved in deionized water. The fully dissolved CTAB solution was added into above alkali-treated HZSM-5 solution and stirred at 60 °C for 1 h. Thereafter, the solution was transferred into a Teflon®-lined stainless-steel autoclave, followed by the first crystallization at 110 °C for 4 h. The pH value of the obtained suspension was then adjusted to be about 8.5 using 2.0 M hydro-

chloric acid solution. The second crystallization was continued at 110 °C for 24 h. During this process, part of the dissolved silicon and aluminum sources formed MCM-41 structure, which was introduced around the undissolved ZSM-5 grains. The precipitates were then separated, washed with distilled water and ethanol, dried, and calcined at 550 °C for 6 h to obtain Na--ZSM-5/MCM-41. Finally, HZSM-5/MCM-41 was then prepared by ion exchange of Na-ZSM-5/MCM-41 using a 1.0 M ammonium chloride solution. The commercial HZSM-5 with SiO_2/Al_2O_3 ratios of 38 and 50 were denoted as HZ-38 and HZ-50, respectively. The real SiO_2/Al_2O_3 ratios of HZSM-5/MCM-41 synthesized using HZ-38 and HZ-50 as starting materials were 36.4 and 39.6, respectively, which were denoted as HZM-38 and HZM-50 based on their starting materials. The decrease of the real SiO_2/Al_2O_3 ratios for HZSM-5/MCM-41 was due to the removal of some silicon species from HZSM-5 molecular sieves by alkali treatment [21,22]. A diagram of the preparation process for HZSM-5/MCM-41 is shown in Figure 1.

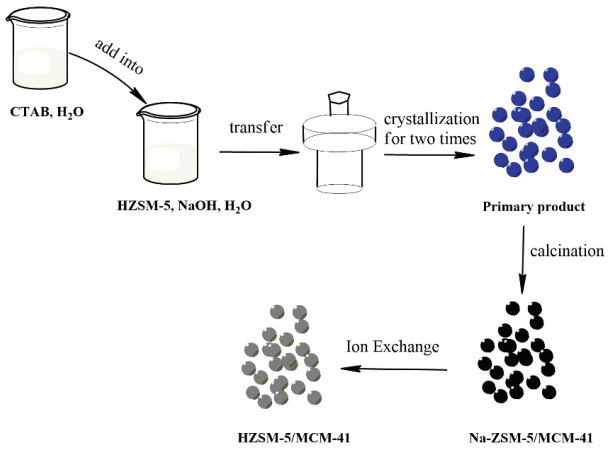

Figure 1. A schematic diagram of the preparation process for HZSM-5/MCM-41.

Characterization

Powder X-ray diffraction (XRD) patterns were recorded on an Ultima IV X-ray diffractometer (40 kV, 40 mA) with a CuK_α radiation source at a scanning rate of 20° min^{-1} from 5 to 80°. Fourier infrared spectroscopy (FTIR) was carried out on a Shimadzu IRAffinity-1s infrared spectrometer in the range of 4000-400 cm^{-1}; the resolution was 4 cm^{-1} and the number of scans was 10 times. The morphology and size of the samples were observed using a JSM--7500F scanning electron microscope (SEM). The N_2--adsorption/desorption analysis was carried out on a BELSORP-MAX specific surface area and pore structure analyzer to characterize the pore structure of the sample. The DFT pore-size distribution of different samples were obtained from the desorption branch. NH_3 temperature-programmed desorption test of the samples was performed on a TP-5076 TPD/TPR dynamic adsorption instrument to characterize the acidity and acid strength of the samples.

Catalytic performance evaluation

1.00 g waste tire and 0.25 g zeolites were mixed evenly and loaded into stainless steel tube, which was then put into the batch reactor. After they were pretreated at 120 °C for 1 h under N_2 atmosphere (30 mL/min), they were heated at a rate of 10 °C min^{-1} to the final temperature of 500 °C, and kept at 500 °C for 1 h. When the temperature reached 400 °C for 1 min, the product stream was injected into two on-line gas chromatographs through two six-port valves and connected by means of a line thermostat at 180 °C to avoid the condensation of heavy products. The total hydrocarbon distribution in terms of the carbon number and the content of monocyclic aromatics and limonene were detected using GC-2014 gas chromatograph equipped with a DB-5MS column (30 m×0.25 mm). However, the C_1-C_4 components could not be effectively separated on the DB-5MS capillary column, so C_1-C_4 hydrocarbons were detected using GC7900 gas chromatograph equipped with a CP7518 column (50 m×0.53 mm). By integrating the above two chromatographic data, a whole component analysis of the pyrolysis product could be obtained.

For all the products injected into gas chromatography, they were artificially divided into C_1-C_4, C_5, C_6, C_7, C_8, C_9-C_{10} and $C_{>10}$ components. The carbon--containing gas phase components (C_1-C_4) in the pyrolysis products would peak in a certain order on the CP7518 capillary chromatographic column. The retention time of each product was obtained using standard substances, so that the corresponding products were qualitatively determined. On the other hand, C_5-$C_{>10}$ components such as monocyclic aromatics and limonene were qualitatively analyzed by obtaining the retention time using the standard substances on the DB-5MS capillary chromatographic column.

The specific calculation process was as follows. First of all, the relative content (Ca(*i*)) of each component of C_1-C_4 was calculated using the peak area of each component in the chromatograph obtained by GC7900, as shown in Eq. (1) (where *fi* is the correction factor, Aa (*i*) and Ab (*i*) are the peak areas of substances in *i* on the GC7900 and GC-2014 chromatographs, respectively):

$$Ca\,(i) = \left[fiAa\,(i)\right)] / [\sum_{i=1}^{4} fiAa\,(i)] \quad (1)$$

Then the relative component content calculated by Eq. (1) was used to distribute the peak area of the peaks (superimposed peaks) of C_1-C_4 components in the GC-2014 chromatograph, as shown in Eq. (2):

$$n_b\,(i) = f_i A_{b(1\text{-}4)} \frac{f_i Aa(i)}{\sum_{i=1}^{4} f_i Aa(i)} \quad (2)$$

Finally, combined with the peak area of C ($n > 4$) components in GC-2014 chromatograph, the content of each component was calculated by area normalization method, as shown in Eq. (3):

$$C_{b\,(i)} = 100 \frac{\sum_{i=1}^{4} nbi}{\sum_{i=1}^{4} nbi + \sum_{i=5}^{n} f_i Abi} = \frac{\sum_{i=1}^{4} Ab(i)}{\sum_{i=1}^{4} nbi + \sum_{i=5}^{n} f_i Ab(i)} \quad (3)$$

For the products in the system, only the hydrocarbons were analyzed. Because their properties were similar, the correction factor (fi) of each component was specified as 1 in the content calculation.

The industrial analysis of waste tire powders proceeded with reference to the industrial analysis method of coal [23]. The elemental analysis of waste tires was carried out on the elemental analyzer of the Elementar Vario MACRO cube. Elemental analysis and industrial analysis results of the waste rubber tires are shown in Table 1.

RESULTS AND DISCUSSION

Structures and morphologies of HZSM-5/MCM-41

The XRD patterns of HZ-38, HZ-50, HZM-38 and HZM-50 zeolites are shown in Figure 2. The peaks between 7 and 10° and between 22.5 and 25° are the characteristic peaks for HZSM-5 molecular sieve, corresponding to the (101), (020), (501), (151) and (303) crystal planes, respectively. It can be seen from Figure 2 that all four samples have five characteristic diffraction peaks of HZSM-5 zeolites. In addition, the XRD patterns in the 2θ of 1-6° for HZM-38 and HZM-50 show the typical MCM-41 structure, with (100), (110) and (200) diffraction peaks appearing at 2θ of about 2.2, 4.1 and 4.6°, respectively. It indicates that HZM-38 and HZM-50 are all HZSM-5/MCM-41 composites. The results show that HZSM-5 is partially dissolved after alkali treatment, while some silicon and aluminum sources dissolved by alkali treatment form MCM-41 structure, which is introduced around the undissolved HZSM-5 grains [24].

SEM images of HZ-38, HZ-50, HZM-38, HZM-50 and γ-Al_2O_3 are shown in Figure 3. The two kinds of

Table 1. Elemental analysis and industrial analysis results of waste rubber tires

Analysis	Elemental analysis					Industrial analysis			
Component	C	H	N	O	S	Moisture	Ash	Volatile	Fixed carbon
Content, wt.%	83.0	5.9	0.6	2.4	1.8	0.84	6.17	56.10	36.89

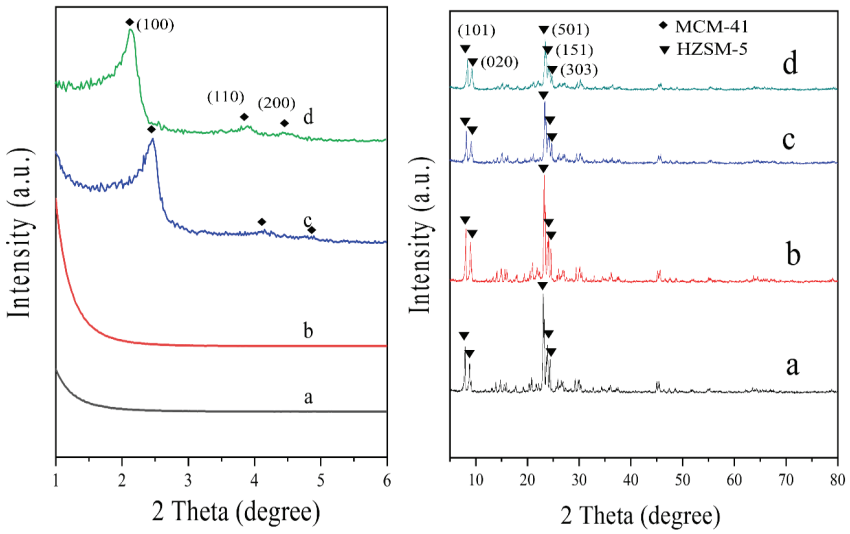

Figure 2. XRD patterns of different zeolites: a) HZ-38; b) HZ-50; c) HZM-38; d) HZM-50.

commercial HZSM-5 catalysts exhibit a hexagonal-like morphology with the size of several micrometers. Similar sizes and more irregular particles are observed for two kinds of HZSM-5/MCM-41 catalysts prepared by alkali treatment of HZSM-5. It can also be seen that the γ-Al_2O_3 have a nonuniform particle size and an unsmooth surface.

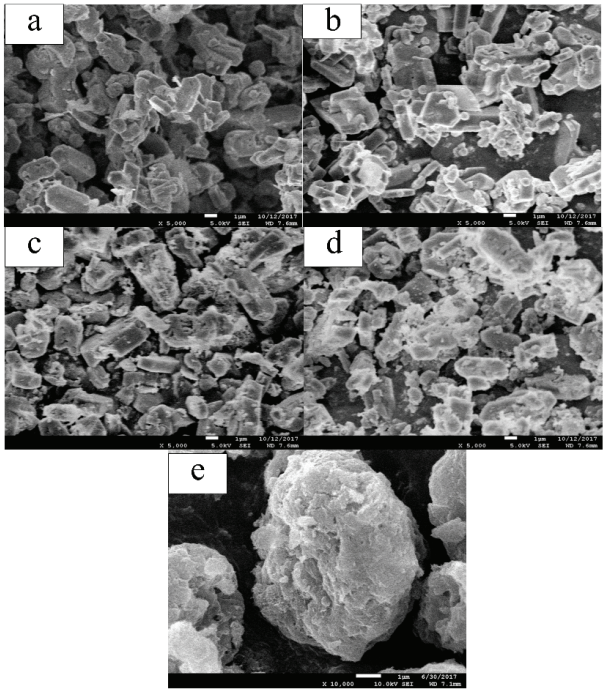

Figure 3. SEM images of different catalysts: a) HZ-38; b) HZ-50; c) HZM-38; d) HZM-50; e) γ-Al_2O_3.

The FTIR spectra of HZ-38, HZ-50, HZM-38 and HZM-50 catalysts are shown in Figure 4. The absorption peak of 1228 cm^{-1} belongs to the in-plane antisymmetric stretching vibration of the five-membered rings. The peaks of 1061 and 793 cm^{-1} are assigned to the out-of-plane antisymmetric stretching vibration and the out-of-plane symmetric stretching vibration of the tetrahedral Si-O-T (T=Si or Al) bond, respectively. The band at 454 cm^{-1} is representing the internal SiO_4 and AlO_4 tetrahedron units [25]. The characteristic peak at 544 cm^{-1} attributed to the vibration peak of five-membered ring structure is a typical peak of MFI catalysts, indicating that all the four samples have the structural units of HZSM-5 catalyst. This is consistent with the results of XRD patterns.

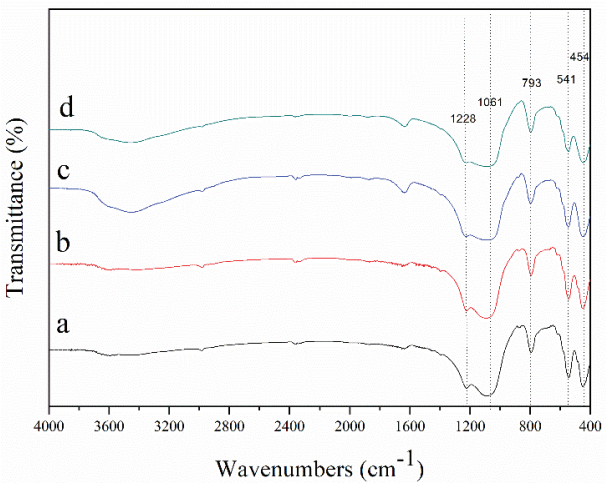

Figure 4. FTIR spectra of different catalysts: a) HZ-38; b) HZ-50; c) HZM-38; d) HZM-50.

Pore structure and acidity of HZSM-5/MCM-41

Figure 5 shows the N_2 adsorption-desorption isotherms of HZ-38, HZ-50, HZM-38 and HZM-50 catalysts. N_2 adsorption-desorption isotherms are related to pore structures of the catalysts. The isotherms of HZ-38 and HZ-50 are type I of typical microporous zeolite catalysts [26], while the isotherms of HZM-38 and HZM-50 show combined characteristics of type I and IV isotherms. The type IV isotherm is the most common adsorption behavior of mesoporous molecular sieves [27], indicating the coexistence of micropores and mesopores. A broad hysteresis loop at the relative pressure of 0.40-0.95 indicates the presence of mesopores in HZM-38 and HZM-50. When the relative pressure is low, the monolayer adsorption of N_2 molecules occurs on the wall of micropores, which makes the isotherm rise linearly. With the increase of relative pressure, the adsorption of N_2 molecules occurs in single-layer and multi-layer adsorption in mesoporous channels. When the relative pressure is increased to 0.40-0.95, the adsorption capacity increases suddenly and an obvious lag loop appears. This is caused by the capillary condensation of N_2 molecules in the mesoporous channels.

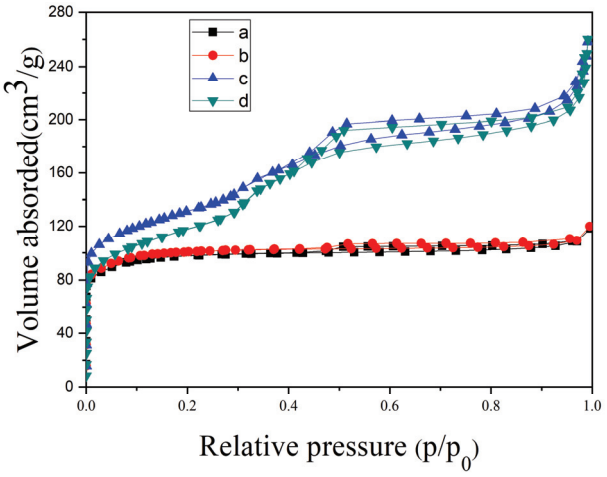

Figure 5. N_2 adsorption-desorption isotherms of different catalysts: a) HZ-38; b) HZ-50; c) HZM-38; d) HZM-50.

Figure 6 shows the pore size distribution of HZ--38, HZ-50, HZM-38, HZM-50 and γ-Al_2O_3 catalysts, and Table 2 shows the structural parameters of the corresponding samples. Compared to HZ-38 and HZ--50, the pore-size distributions of HZM-38 and HZM--50 indicate the coexistence of mesopores and micropores, confirming the presence of mesopores. It can also be seen from Table 2 that the two kinds of HZSM-5/MCM-41 catalysts have larger specific surface areas (418.7 and 468.5 m^2/g) than the two HZSM-5 catalysts (373.2 and 386.6 m^2/g) due to the introduction of mesoporous MCM-41. In addition to the specific surface area, the total pore volume also obviously increases for HZM-38 and HZM-50. As shown in Figure 6e, both mesopores and macropores are found to be present in γ-Al_2O_3.

The NH_3-TPD profiles of HZ-38, HZ-50, HZM--38, HZM-50 and γ-Al_2O_3 catalysts are shown in Figure 7. The peak shape of HZ-38 and HZ-50 is consistent with that of HZSM-5 catalyst reported in the literature [28], the peak at 100-310 °C is assigned to weak acid site, and the peak at 310-600 °C is assigned to strong acid site [29]. γ-Al_2O_3 is recognized as a solid acid catalyst without strong acid sites, therefore there is a broad and low desorption peak for the NH_3--TPD curve of γ-Al_2O_3. Compared to HZ-38 and HZ--50, the peaks of strong acid site for HZM-38 and HZM-50 decrease obviously. This indicates that the strong acid sites of HZM-38 and HZM-50 are less than those of HZ-38 and HZ-50. During the process of alkali treatment of HZSM-5 molecular sieve, part of Al is dissolved from the skeleton structure of HZSM-5 molecules and participates in the formation of MCM--41, resulting in the conversion of some B acid sites to L acid sites [20].

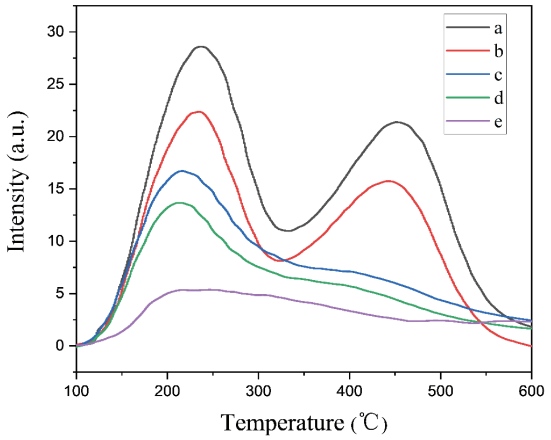

Figure 7. NH_3-TPD profiles of different catalysts: a) HZ-38; b) HZ-50; c) HZM-38; d) HZM-50; e) γ-Al_2O_3.

For zeolites, the total acid content decreases with the increase of SiO_2/Al_2O_3 ratio. As shown in

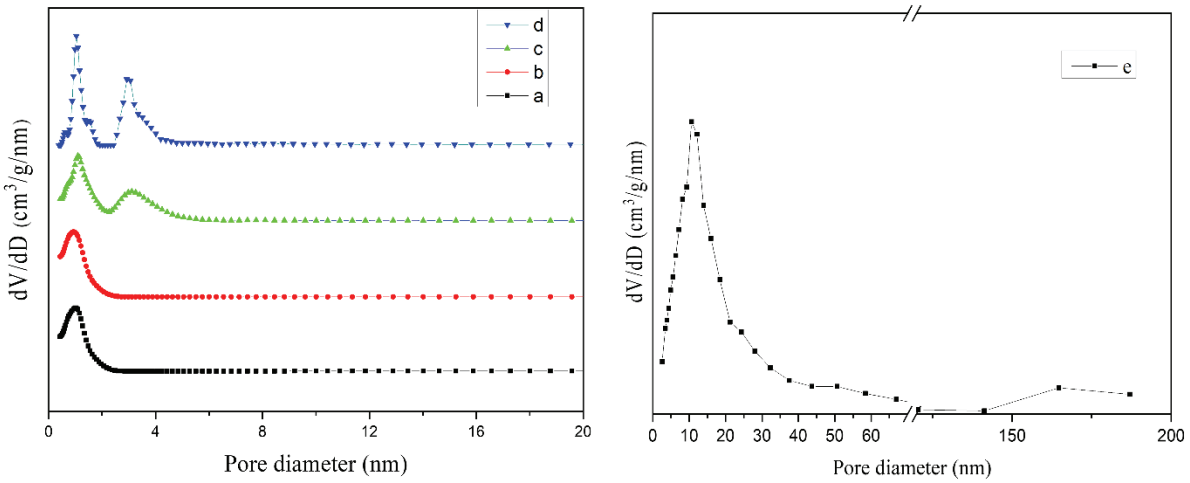

Figure 6. Pore size distribution of different catalysts: a) HZ-38; b) HZ-50; c) HZM-38; d) HZM-50; e) γ-Al_2O_3.

Table 2. Structure parameters of different catalysts

Sample	S_{BET}[a] (m^2/g)	V_{total}[b] (cm^3/g)	Dp_{micro}[c] (nm)	Dp_{meso}[d] (nm)	Dp_{macro}[e] (nm)
HZ-38	373.2	0.180	0.94	-	-
HZ-50	386.6	0.182	0.96	-	-
HZM-38	418.7	0.388	1.05	3.32	-
HZM-50	468.5	0.292	1.06	3.35	-
γ-Al_2O_3	263	1.28	-	11.81	166.20

[a]BET surface area; [b]total pore volume; [c]average micropore diameter; [d]average mesopore diameter; [e]average macropore diameter

Table 3, HZ-50 and HZM-50 exhibit the less total acid contents than HZ-38 and HZM-38, respectively, due to the higher SiO_2/Al_2O_3 ratios [30,31]. However, for HZSM-5/MCM-41catalysts, their total acid content is much lower than that of HZSM-5 catalyst with the same SiO_2/Al_2O_3 ratio. Because of alkali treatment, part of the HZSM-5 structure is destroyed, therefore the total acid content especially the amount of strong acid sites obviously decreases.

Catalytic performances of different catalysts

Considering some characteristics of macroporous γ-Al_2O_3, such as large specific surface area (Table 2, 263 m^2/g), larger pore diameter (Figure 6, pore size distribution of 5-70 nm), and a certain amount of acid sites (Figure 7 and Table 2, 131.18 μmol/g), 0.5 g of γ-Al_2O_3 were added into 0.25 g of HZSM-5/MCM-41 to obtain the mixed catalysts with micro-, meso- and macropores to catalyze the pyrolysis of waste tires. The mixture of γ-Al_2O_3 and HZM--38 (or HZM-50) were named as HZM+A-38 (or HZM++A-50). In order to confirm the role of γ-Al_2O_3, 0.5 g of inert SiO_2 was mixed with 0.25 g HZM-50 to catalyze the pyrolysis of waste tires. The mixture of SiO_2 and HZM-50 was named as HZM+S-50.

The catalytic performances of γ-Al_2O_3, HZM-38, HZM-50, HZM+A-38, HZM+A-50 and HZM+S-50 for the pyrolysis of waste tires are shown in Figure 8. The product selectivities for thermal pyrolysis of waste tires is also displayed in Figure 8. As shown in Figure 8A, the pyrolysis products include different hydrocarbons from C_1 to $C_{>10}$. In Figure 8B, the selectivity of

Table 3. Acid content distribution of different catalysts

Sample	Total acid content, μmol/g	Weak acid amount, μmol/g	Strong acid amount, μmol/g
HZ-38	569.10	265.77	303.33
HZ-50	441.17	204.75	236.42
HZM-38	286.55	142.10	144.45
HZM-50	229.26	115.07	114.19
γ-Al_2O_3	131.18	72.07	59.11

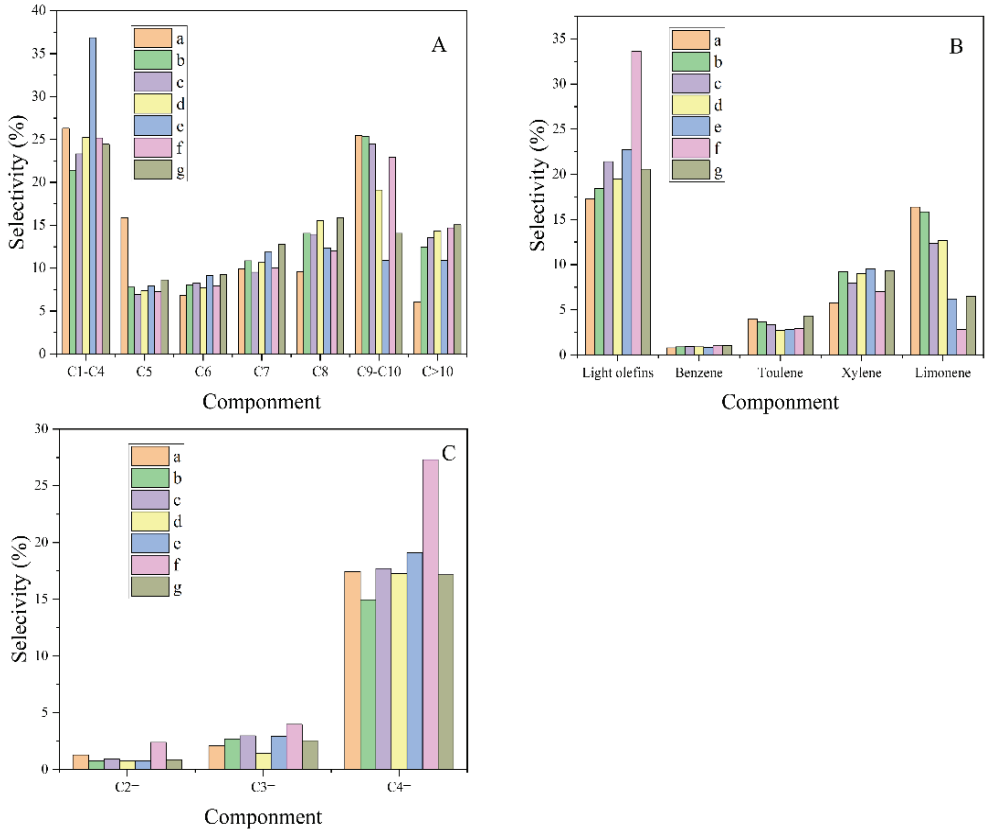

Figure 8. Effect of different catalysts on the catalytic performances for the pyrolysis of waste tires: a) non-catalysts; b) HZM-38; c) HZM-50; d) γ-Al_2O_3; e) HZM+A-38; f) HZM+A-50; g) HZM+S-50.

light olefins without catalysts is the lowest, which is 17.27%. The selectivities of light olefins for γ-Al_2O_3, HZM-38 and HZM-50 are 19.50, 18.43 and 21.42%, respectively. The selectivities of light olefins for HZM+ +A-38 and HZM+A-50 are 22.74 and 33.65%, respectively, higher than corresponding HZM-38 and HZM-50. HZM+A-50, the mixture of γ-Al_2O_3 and higher SiO_2/Al_2O_3 HZSM-5/MCM-41, shows the highest light olefin selectivity. This indicates that the selectivity of light olefins is significantly improved due to the introduction of macroporous γ-Al_2O_3 into hierarchical HZSM-5/MCM-41 with micro- and mesopores. As shown in Figure 8C, the selectivities of ethylene are almost the same. The source of ethylene may be due to olefin cracking in the range of gasoline. Ethylene as the primary product of waste tire cracking in the presence of zeolite catalysts is kinetically unfavorable because the formation of ethylene involves relatively unstable primary carbene ion intermediates, and changes of C_2-gases are not always be observed by lower levels of catalysts. The selectivity of propylene is improved to some extent. The addition of catalysts increases the effective cracking/hydrogen transfer ratio because it mainly acts on the cracking of higher olefins to C_3-C_5 olefins [32]. In addition, C_4 olefins are dominant in the light olefins; this may be attributed to the fact that the main component of the tire is styrene-butadiene rubber (SBR) [33].

As can be seen from Figure 8B, the selectivities of "BTX" (benzene, toluene, xylene) for γ-Al_2O_3, HZM- -38, HZM+A-38, HZM-50 and HZM+A-50 are 12.65, 13.77, 13.16, 12.26 and 10.96%, respectively. While the selectivity of "BTX" is 10.56% in the case of waste tire thermal pyrolysis. HZM-50 shows lower "BTX" selectivity than HZM-38, and HZM+A-50 exhibits lower "BTX" selectivity than HZM+A-38. This indicates that the catalysts with higher SiO_2/Al_2O_3 ratios do not benefit the production of aromatic hydrocarbons due to their lower acid density. In addition, the introduction of γ-Al_2O_3 can also decrease the selectivity for "BTX". Compared with the selectivity of light olefins for waste tire pyrolysis using different catalysts, higher SiO_2/ /Al_2O_3 ratio of HZSM-5/MCM-41 and their mixtures with γ-Al_2O_3 show higher light olefin selectivity and lower "BTX" selectivity. During the process of waste tire pyrolysis, as-produced ethylene and propylene are further converted to aromatics at acid sites by aromatization and Diels-Alder reaction [34] due to the pore size constraint and higher acid density. Because the diffusion of light olefins is not easy in the long and narrow micropores, as-obtained light olefins continue to react at acid sites in the pores to produce aromatics [13,14]. Furthermore, the higher acid density also makes the resulting light olefins continue to react at strong acid sites to produce aromatics [15,16]. After macroporous γ-Al_2O_3 is mixed with HZSM-5/ /MCM-41, the acidity and the pore size constraint decrease to some extent. Therefore, the light olefin selectivity increases and the "BTX" selectivity decreases. In addition, lower SiO_2/Al_2O_3 ratio of HZSM-5/ /MCM-41 has higher acid density, as-obtained light olefins can also react at close acid sites to form aromatics. That is why HZM-38 (SiO_2/Al_2O_3: 36.4) show lower light olefin selectivity and higher "BTX" selectivity than HZM-50 (SiO_2/Al_2O_3: 39.6). Therefore the mixture of higher SiO_2/Al_2O_3 ratio of HZSM-5/MCM-41 and γ-Al_2O_3 show the highest light olefin selectivity and the lowest "BTX" selectivity due to the lower acid density as well as improved pore size constraint.

As can be seen from Table 4, there are some reports on HZSM-5/MCM-41 composites used as catalysts for pyrolysis of rice husk and n-decane. Other molecular sieves such as HZSM-5, HY and HY/MCM- -41 are reported as catalysts for pyrolysis of tire

Table 4. Light olefin selectivity/yield/concentration/relative abundance of waste tire cracking using different catalysts; S/Y/C/RA: S - selectivity; Y - yield; C - concentration; RA - relative abundance

No.	Catalysts	Raw material	S/Y/C/RA	Ref.
1	HZSM-5/MCM-41	Waste tire	Light olefins 21.42%(S)	This work
	HZSM-5/MCM-41+γ-Al_2O_3		Light olefins 33.65%(S)	
2	HZSM-5	Polybutadiene rubber	Olefins 16.8%(Y)	[9]
3	USY	Waste tire	Olefins 4.25%(C)	[10,11]
	HZSM-5		Olefins 27.26%(C)	
4	Ru/MCM-41	Tire	Light olefins 7.6%(Y)	[1,17]
	Ru/MCM-48			
5	HY/MCM-41	Waste tire	Olefins 12.0%(Y)	[18]
6	HZSM-5/MCM-41	Rice husk	Olefins 14.5%(RA)	[19]
7	HZSM-5/MCM-41	n-decane	Light olefins 21%(S)	[20]
8	nano-HZSM-5/γ-Al_2O_3	Waste tires	Light olefins 29.9%(S)	[37]
9	Used catalyst	Waste tire	Propene and 1-butene 18.25%(Y)	[38]

wastes. In the catalytic cracking of waste tires or other polymers, the mixture of γ-Al_2O_3 and HZSM-5/MCM-41 in this work shows the highest selectivity of light olefins compared with other studies. This may be due to the unique composition and micro-, meso- and macroporous structure of the catalysts.

Limonene is the main component of C_9-C_{10}. The selectivities of limonene for HZM-38, HZM-50, HZM++A-38 and HZM+A-50 are 15.87, 12.37, 6.22 and 2.85%, respectively. The lowest limonene selectivity is obtained using HZM+A-50 catalysts. Unlike other reports on pyrolysis and catalytic reforming of volatile components [10,11,35], with the presence of HZSM-5 catalyst, limonene is mainly converted to aromatic compounds [36]. The yield of limonene depends on the strength and density of acid sites and the pore structure of acid catalysts [39]. Compared with HZSM-5/MCM-41 composite catalysts, the selectivity of light olefins can be improved by adding γ-Al_2O_3. The increase of selectivity of gas products is at the cost of reducing the selectivity of liquid products. Therefore, it can also be seen from the figure that the selectivity of liquid products has been reduced to a certain extent, especially the selectivity of limonene, which has decreased by about 10%.

As shown in Figure 8B, the selectivity of light olefins for the pyrolysis of waste tires using HZM+A-38 as catalysts can be partially improved with the introduction of γ-Al_2O_3 compared with HZM-38 molecular sieves. However, it is much lower than that of HZM+A-50 catalysts. This further illustrates the importance of appropriate acid strength and acid content for catalytic cracking waste rubber tires to obtain higher selectivity of light olefins. Compared with HZM-50 zeolites, the selectivity of light olefins obtained using HZM+S-50 nearly does not change, except for limonene. In addition, compared with HZM+S-50, the selectivity of light olefins for HZM+A-50 is obviously higher, indicating that the large pore size, high specific surface area and suitable acid content of γ-Al_2O_3 play an important role in obtaining higher selectivity of light olefins.

CONCLUSIONS

Compared with HZSM-5 catalyst, the micro-mesoporous HZSM-5/MCM-41 catalyst has larger pore diameter, larger specific surface area and lower total acid content. When HZSM-5/MCM-41 is used as the catalyst, the selectivity of light olefins for HZM-50 (21.4%) is higher than that of HZM-38, while the HZM-38 can obtain higher selectivity of “BTX”. The selectivity of light olefins can be improved by adding γ-Al_2O_3. When HZM+A-50 is used as catalyst, the selectivity of light olefins is 33.6%, which is much higher than that of 21.4% without γ-Al_2O_3. It is of great practical significance to use waste tires as the production resource of light olefins.

Acknowledgments

The authors of this paper would like to thank the Analysis & Testing Center, Beijing Institute of Technology for sponsoring this research. This research was also supported by Beijing Key Laboratory for Chemical Power Source and Green Catalysis, Beijing Institute of Technology.

REFERENCES

[1] D.N. Anh, K. Raweewan, W. Sujitra, J. Sirirat, J. Anal. Appl. Pyrolysis 86 (2009) 281-286

[2] J.M. Lee, J.S. Lee, Energy 20 (1996) 969-976

[3] G. Lopez, M. Olazar, M. Amutio, R. Aguado, J. Bilbao, Energy Fuels 23 (2009) 5423-5431

[4] P.T. Williams, Waste Manage. 33 (2013) 1714-1728

[5] A.M. Fernández, C. Barriocanal, R. Alvarez, J. Hazard. Mater. 203-204 (2012) 236-243

[6] J.P. Falkenhagen, L. Maisonneuve, P.P. Paalanen, N. Coste, N. Malicki, B.M. Weckhuysen, Chem.Eur.J. 24 (2018) 4597-4606

[7] S. Abbasizadeh, R. Karimzadeh, Ind. Eng. Chem. Res. 57 (2018) 7783-7794

[8] K. Sana, P. Maria, T. Mohand, K. Besma, Z. Fethi, J Energy Resour. Technol. 139 (2016) 032203

[9] S.S.Z. Salmasi, M.S. Abbas-Abadi, M.N. Haghighi, H. Abedini, Fuel 160 (2015) 544-548

[10] B. Shen, C. Wu, C. Liang, B. Guo, R. Wang, J. Anal. Appl. Pyrolysis 78 (2007) 243-249

[11] B. Shen, C. Wu, B. Guo, R. Wang, C. Liang, Appl. Catal., B 73 (2007) 150-157

[12] G.S. Miguel, J. Aguado, D.P. Serrano, J.M. Escola, Appl. Catal., B 64 (2006) 209-219

[13] J. Zheng, Q. Zeng, Y. Yi, Y. Wang, J. Ma, B. Qin, X. Zhang, W. Sun, R. Li, Catal. Today 168 (2011) 124-132

[14] J. Shah, M.R. Jan, F. Mabood, Energy Convers. Manage. 50 (2009) 991-994

[15] S. Kotrel, H.G.C. Knozinger Microporous Mesoporous Mater. 35-36 (2000) 11-20

[16] X. Li, B. Shen, C. Xu, Appl. Catal., A 375 (2010) 222-229

[17] C. Witpathomwong, R. Longloilert, S. Wongkasemjit, S. Jitkarnka, Energy Procedia 9 (2011) 245-251

[18] W. Namchot, S. Jitkarnka, J. Anal. Appl. Pyrolysis 121 (2016) 297-306

[19] Z. Li, Z. Zhong, B. Zhang, W. Wang, W. Wu, J. Anal. Appl. Pyrolysis 138 (2019) 103-113

[20] Y. Sang, Q. Jiao, H. Li, Q. Wu, Y. Zhao, K. Sun, J. Nanopart. Res. 16 (2014) 2755

[21] T. Fu, R. Qi, W. Wan, J. Shao, J.Z. Wen, Z. Li, ChemCatChem 9 (2017) 4212-4224

[22] Z. Ma, T. Fu, Y. Wang, J. Shao, Q. Ma, C. Zhang, L. Cui, Z. Li, Ind. Eng. Chem. Res. 58 (2019) 2146-2158

[23] R.A. Nadkarni, Anal. Chem. 52 (1980) 929-935

[24] H. Li, S. He, K. Ma, Q. Wu, Q. Jiao, K. Sun, Appl. Catal., A 450 (2013) 152-159

[25] F.G. Denardin, O.W. Perez-Lopez, Microporous Mesoporous Mater. 295 (2020) 109961

[26] Y.F. Yeong, A.Z. Abdullah, S.B.A. Latif Ahmad, Microporous Mesoporous Mater. 123 (2009) 129-139

[27] Y. Luo, P. Yang, J. Lin, Microporous Mesoporous Mater. 111 (2008) 194-199

[28] K. Ding, Z. Zhong, B. Zhang, J. Wang, A. Min, R. Ruan, J. Anal. Appl. Pyrolysis 122 (2016) 55-63

[29] Y. Gu, N. Cui, Q. Yu, C. Li, Q. Cui, Appl. Catal., A 429-430 (2012) 9-16

[30] A.S. Al-Dughaither, H. de Lasa, Ind. Eng. Chem. Res. 53 (2014) 15303-15316

[31] D. Ma, W. Zhang, Y. Shu, X. Liu, Y. Xu, X. Bao, Catal. Lett. 66 (2000) 155-160

[32] Y.G.A.J. Scott Buchanan, Appl. Catal., A 134 (1996) 247-262

[33] C. Berrueco, E. Esperanza, F.J. Mastral, J. Ceamanos, P. García-Bacaicoa, J. Anal. Appl. Pyrolysis 74 (2005) 245-253

[34] S. Muenpol, R. Yuwapornpanit, S. Jitkarnka, Clean Technol. Environ. Policy 17 (2016) 1149-1159

[35] M. Olazar, M. Arabiourrutia, G. López, R. Aguado, J. Bilbao, J. Anal. Appl. Pyrolysis 82 (2008) 199-204

[36] M. Arabiourrutia, M. Olazar, R. Aguado, G.L. Pez, A. Barona, J. Bilbao, Ind. Eng. Chem. Res. 47 (2008) 7600-7609

[37] Z. He, Q. Jiao, Z. Fang, T. Li, C. Feng, H. Li, Y. Zhao, J. Anal. Appl. Pyrolysis 129 (2018) 66-71

[38] C. Wang, X. Tian, B. Zhao, L. Zhu, S. Li, Processes 7 (2019) 335.

RURU FU[1]
ZHUANGZHANG HE[1]
SHIKAI QIN[1]
QINGZE JIAO[1,2]
CAIHONG FENG[1]
HANSHENG LI[1]
YUN ZHAO[1]

[1]School of Chemistry and Chemical Engineering, Beijing Institute of Technology, Beijing, PR China
[2]School of Materials and Environment, Beijing Institute of Technology, Zhuhai, Guangdong, PR China

NAUČNI RAD

PROIZVODNJA LAKIH OLEFINA KORIŠĆENJEM SMEŠE HZSM-5/MCM-41 I γ-Al_2O_3 KAO KATALIZATORA ZA KATALITIČKU PIROLIZU OTPADNIH GUMA

U ovom radu, mikro-mezoporozni HZSM-5/MCM-41 zeoliti pripremljeni su dvostepenom hidrotermičkom metodom koristeći komercijalni HZSM-5 sa dva različita odnosa silika/ /glinica (38 i 50) kao polaznim materijalima. Strukture, morfologije i kiselost pripremljenih zeolita analizirani su korišćenjem KSRD, FT-IR, SEM, N_2-adsorpcija/desorpcija i NH_3-TPD. Zeoliti HZSM-5/MCM-41 kombinovali su kiselost mikroporoznog HZSM-5 sa prednostima pora mezoporoznog MCM-41. Utvrđeno je da su mezopore i mikrospore sa prečnikom od 3,34 i 0,95 nm prisutne u zeolitima HZSM-5/MCM-41. Kada su korišćeni za katalizu pirolize otpadnih guma, selektivnost lakih olefina za HZSM-5/MCM-41 pripremljenih korišćenjem HZSM-5 sa odnosom silika /glinice 50 kao početnih materijala iznosila je 21,42%, što je više od 18,43% ostvarenog sa HZSM-5 / MCM-41 koji je sintetizovan pomoću HZSM-5 sa odnosom silika/glinica od 38. Da bi se dalje prevazišla ograničenja veličine pora i ograničenja prenosa mase zeolita HZSM-5/MCM-41 za katalizu pirolizu otpadnih guma, makroporozni g-Al_2O_3 je pomešan sa HZSM-5/MCM-41 i korišćen kao katalizator. Selektivnost prema lakim olefinima za smešu γ-Al_2O_3 i HZSM-5/MCM-41, koji je pripremljen upotrebom HZSM-5 sa odnosom silika/glinice od 50 kao polaznih materijala, iznosila je 33,65%, što je očigledno poboljšannje.

Ključne reči: katalitička piroliza; HZSM-5; laki olefini; MCM-41; Otpadne gume. γ-Al_2O_3.